IMPROVING 3D SURFACE MEASUREMENT OF MECHANICAL DETAILS BY STRUCTURED LIGHT USING HIGH DYNAMIC RANGE

Nguyen Ngoc Tu[1*], Nguyen Thi Phuong Mai[1], Nguyen Van Thuong[2], Doan Van Tuan[3]

Abstract: *The measurement methods using structured light have the advantage of being fast, accurate, and noncontact with the surface of the object. However, these methods have reached its limitation when measuring mechanical details with high surface gloss, due to the unpredictable reflection of incident rays after reaching to object's surface that, consequently, leads to the simultaneous appearance of several regions with different brightness. To address this problem, we proposed a method of synthesizing extended dynamic range images based on changing the exposure time of the camera and adjusting the illumination of the projector light source so that 3D point coordinates in both bright and dark areas could be obtained through the process. The dual-camera structured light experimental model and the lightcrafter 4500 projector are synchronized through the trigger, using the gray code in combination with the line-shift projection pattern. Experimental results show that the proposed method can precisely reconstruct the 3D surface of mechanical details, while providing higher performance than the state-of-the-art methods.*

Keywords: Structured light; Gray code; Line-shift; 3D Measurement System; HDR.

1. INTRODUCTION

The 3D optical measurement technique based on the non-contact measurement method has an important role in the industrial inspection of manufactured parts, reverse engineering (digitization of complex, free-form surfaces), object recognition, entertainment, 3D map building, biometrics, and documentation of cultural artifacts [1-4]. Currently, the methods of using structured light have many outstanding advantages such as high resolution, measurement for the entire sampling range, fast data acquisition time. Thus, they are extremely useful when used with free and complex surfaces that require no contact between external tools and the sample. Typically, a structured light measurement system consists of a camera and a projector that projects a sequence of coded patterns onto object surfaces. The camera is responsible for capturing the textures on the surface of the object from another direction. Then, from the captured images, the absolute phase map is obtained using a specially designed algorithm, such as a phase-shifting algorithm. Finally, the 3D coordinates of the object surface can be calculated from the absolute phase map using a phase-to-height mapping based on a calibration performed earlier over the measurement volume of interest.

However, the use of this system still involves difficulties when dealing with nondiffuse (non-Lambertian) surfaces because the optical signal cannot be properly retrieved. Most optical measurement methods require the surface of the object being measured is a Lambertian surface, which has a diffuse or near-diffuse reflectance and low reflectivity variations from point to point. In detail, the object surface which receives the direct light is exposed to the glare (exceeding the threshold of 0 ~ 255 gray level intensity range of the camera) is always ON and cannot distinguish between projection bits. Besides, the surface parts which completely reflected in the other direction compared with the camera position are dark and the bit of projection is always OFF. To address these problems, several methods, which can measure the glossy surfaces, have been proposed, called High Dynamic Range (HDR) technique. The HDR 3D shape measurements techniques can be divided into six categories [5-12]: (1) using multiple exposures; (2) adjusting projected pattern intensities; (3) using polarizing filters; (4) using color invariants; (5) photometric stereo technique; and (6) miscellaneous.

Each method has its advantages and disadvantages depending on the characteristics and complexity of the measuring system. By exploiting the advantage of clearly distinguishing the bits with sub-pixel accuracy, in this paper, we present the studies related to the 3D surface acquisition of mechanical parts using gray code and line-shift methods, along with improving the quality of data measured using HDR image synthesis techniques.

2. PROPOSED METHOD

2.1. Principle of 3D acquisition method

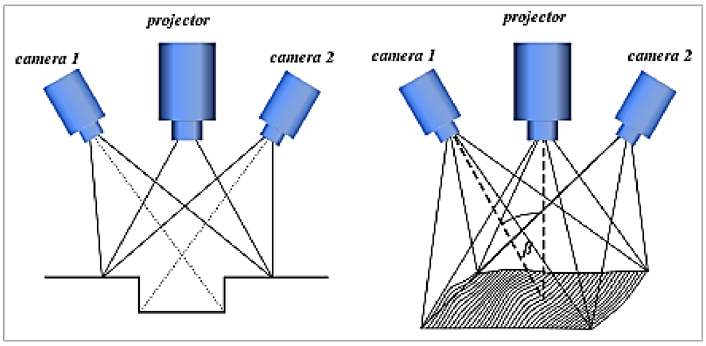

Figure 1. *Gray code and line shifting measurement system using two cameras camera and one projector.*

Fig. 1 shows the 3D image acquisition system, which includes a projector to project textured patterns coded by the structured light method. The used pattern is gray code combined with line-shift. Two cameras are able to capture pictures of ridges on reflections on the object surface, similar to a stereo camera system.

The set of pattern images obtained from two cameras will be decoded, then find a pair of similarities according to the encoded coordinate value between two cameras, apply triangulation to calculate each 3D point coordinate on the object surface.

2.2. The structure of the projection system for the gray code and line-shift method

Gray code is generated to produce patterned images and the order observes the gray code. Assume we project an $W \times H$ image (W and H is the width and height of the image, respectively) and the patterns are generated following row and column. The number of bit N is first computed to encode the pixel per row-column. N is obtained as

$$N \geq log_2(W) \quad (1)$$

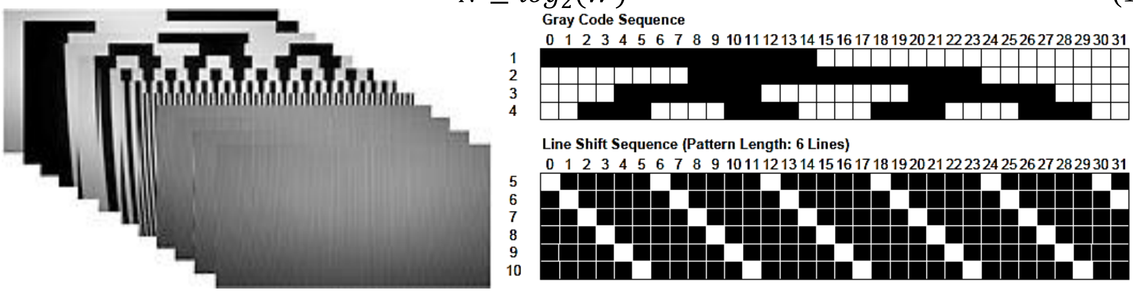

Figure 2. *Gray code 10bit patterns and line-shifting.*

Fig. 2 shows assuming that the image has a width of 1024 pixels, so we need $N = log2(1024) = 10$ bit to encode these pixels, respectively. We project 10 images corresponding to 10 bits, so each pixel column will be encoded by a gray code corresponding to the position of that column. To generate a line-shift pattern, a line pattern with a pixel width of 1 pixel is used, between the lines is 6 or 8 pixels in x and y directions, respectively.

2.3. Lighting component identification from projector

In 2D images that the cameras obtained during projection, [13] introduced an analysis of the gray-level composition including the magnitude of the light from the projector and external environmental components.

a) b)

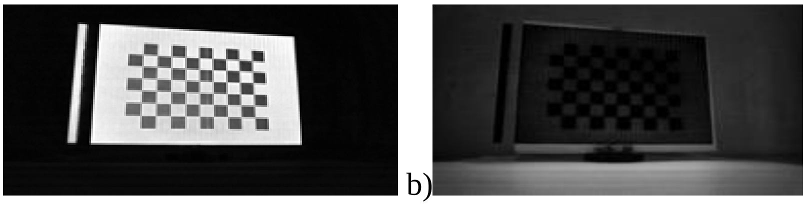

Figure 3. *Bright image from (a) projector, (b) environment.*

To determine the lighting value at points within the projector's working area, assuming that we have $S = \{I_1, I_2, \dots, I_k\}$ is a set of pattern images, where each pixel p in the image is defined as "direct" (L_d) and "general" (L_g). $L_d(p)$, $L_g(p)$ are defined as:

$$L_p^+ = \max_{0<l\le k}\big(I_l(p)\big),\ L_p^- = \min\big(I_l(p)\big) \quad (2)$$

$$L_d(p) = \frac{L_p^+ - L_p^-}{1-b}, \qquad L_g(p) = 2\frac{L_p^- - bL_p^+}{1-b^2} \quad (3)$$

Where $b \in [0, 1]$ is the light information modeling value transmitted by turning off the pixels of projector.

2.4. ON-OFF classification

The light composition of an image after the pixel classification [13] consists of three distinct levels: ON is the pixel of the bright pattern, OFF is the pixel of the dark pattern, and Uncertain is the uncertain element which can be ON or OFF pixel, this part can be a shadow of an object or a dark object, etc. For un-illuminated pixels, its gray density p contains only the non-direct light component i_{off} and p is represented as

$$p = \begin{cases} d + i_{on} & \text{if pixel } ON \\ i_{off} & \text{if pixel } OFF \end{cases} \quad (4)$$

Where: + Indirect light composition: $i_{total} = i_{on} + i_{off}$;

+ Light composition d and i_{total} are computed using Nayar's separation method.

To segment the pixels, [14] gives the following definition:

- $d < m$: pixel is UNCERTAIN;
- $p < \min(d, i_{total})$: pixel is OFF;
- $p > \max(d, i_{total})$: pixel is ON ;
- In contrast, pixel is UNCERTAIN.

Where m is the minimum threshold defined for distinguishing pixel shadows of the object.

2.5. Lighting line top determination

The line-shift method is proposed to improve the gray code. By replacing the even value of the points coordinates on the camera from pixels down to the sub-pixel, the vertices of the projections are not above the position of the original pixel. The value is a real number so the point cloud accuracy is better. [1] introduced a method using detectors that are independent of ambient light, which can be applied for group 4 or 8:

$$g_4(i) = f(i-2) + f(i-1) - f(i+1) - f(i+2) \quad (5)$$

$$g_8(i) = f(i-4) + f(i-3) + f(i-2) + f(i-1) - f(i+1) - f(i+2) - f(i+3) - f(i+4) \quad (6)$$

Where: $f(i)$ is the gray level value of the image at the pixel in the i .th column; $i \in \{0, \dots, W\}$; W is the width value of the image.

Thus, the central position of the sub-pixel vertex is determined by linear interpolation intersecting with the characteristic line 0.

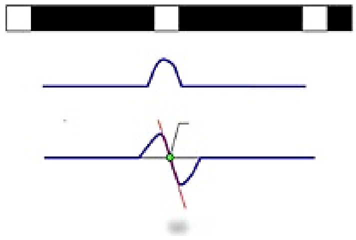

Figure 4. *The sub-pixel position using linear interpolation.*

2.6. Pixel distance determination using approximation method

After obtaining the corresponding coordinates between the pixels on the camera and the projector (the decoded image and the coordinates camera row-column from line-shift) along with the system parameters, the final step is to determine the z value of the pixel with the assumption of finding the intersection point of two lines given the origin and the direction vector. In this step, we follow the approximation method for two intersection lines

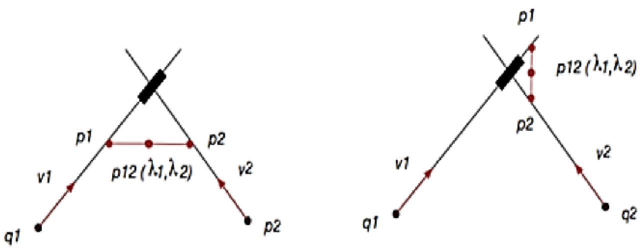

Figure 5. *Approximation method for two intersection lines.*

In Fig. 5, p_{12} is the unknown point with coordinates x, y, z, where z is the distance from the pixel to the acquisition system.

q_1 and q_2 are the origin of the pixels on the projector and the camera, respectively. p_1 and p_2 are the points after decoding, where p_1 were performed multiplication with the rotation matrix R and p_2 is the result of the decode point after performing subtraction with the translation matrix T and multiplication with the rotation matrix R. p_{12} is obtained as:

$$p_{12} = p_1 + \frac{1}{2}(p_2 - p_1),\ p_1 = q_1 + \lambda_1 v_1, \qquad p_2 = q_2 + \lambda_2 v_2 \tag{7}$$

$$\begin{pmatrix} \lambda_1 \\ \lambda_2 \end{pmatrix} = \begin{pmatrix} \|v_1\|^2 & -v_1^i v_2 \\ -v_2^i v_1 & \|v_2\|^2 \end{pmatrix}^{-1} \begin{pmatrix} v_1^i(q_2 - q_1) \\ v_2^i(q_1 - q_2) \end{pmatrix} \tag{8}$$

Where: λ_1, λ_2 is the unit coefficient of vector v_1 and v_2.

2.7. HDR technique for gray code and line-shift

For current HDR methods, the authors primarily apply the phase shift projection method with the feature of selecting exposure values at different gray levels, so it is difficult to apply to the gray code and line-shift method. In this section, we proposed a simple method to synthesize depth images and produce the high-quality 3D image for high-gloss objects.

Assuming that each pixel in the image obtained from the initial camera has a gray level value of $I_0(x, y)$, where x and y are the coordinates of the row and column position of a pixel, respectively. When increasing the exposure value of the camera, the gray level in the high-gloss surface area will quickly reach the saturation state (the maximum value of the pixel is 255). If continue to increase the exposed value, the low-gloss areas or large angles will be simultaneously increased and gradually saturation value. Thus, the aggregate function can be obtained as:

$$I_{HDR-i-(x,y)} = \sum_{i=0}^{n} \frac{t_0}{t_i} \times I_{i(x,y)} \quad (9)$$

Where: (x, y) is the pixel position in row and column ($x \in \{0, Image_{Width}\}$; $y \in \{0, Image_{Height}\}$), respectively; I is the pixel value. The pixel value is normalized from [0-255[to [0-1] to increase the range amplitude and we set $I_{i(x,y)} \leq 0.99$.

3. EXPERIMENTAL RESULT

3.1. System configuration

The system includes two cameras, one projector and one computer as shown in Fig. 6. The distance between the camera and the projector is 70 mm.

+ Projector: DLP LED lighting technology, the resolution (912×1140) pixels, 1000 lumen.

+ Camera: 02 Camera FLIR Grasshopper USB 3.0: The resolution (2048×1536) pixels, 121 fps, global shutter.

+ Lens: f = 8 mm, field of view (DHV): 67.10° × 56.30° × 43.70°.

***Figure 6**. The proposed scan 3D automatic system.*

The system is calibrated on the optical table, using a 11×8 chessboard with a plot size of (7×7) mm, to find the rotation matrix R and transfer vector T between two cameras, the internal calibration parameters K_c of the camera is

- Camera 1: $K_c = \begin{bmatrix} 2.3387e+03 & 0 & 1024 \\ 0 & 2.3387e+03 & 768 \\ 0 & 0 & 1 \end{bmatrix}$,

  $K = [-2.4116e-01 \quad 2.6726e-01 \quad 0 \quad 0 \quad 0]$
- Camera 2: $K_c = \begin{bmatrix} 2.3432e+03 & 0 & 1024 \\ 0 & 2.3432e+03 & 768 \\ 0 & 0 & 1 \end{bmatrix}$

  $K = [-2.29261e-01 \quad 1.8543e-01 \quad 0 \quad 0 \quad 0]$
- Rotation matrix R: $R = \begin{bmatrix} 9.20e-01 & -3.60e-03 & 3.90e-01 \\ 6.50e-03 & 9.99e-01 & -6.09e-03 \\ -3.98e-01 & 8.14e-03 & 9.20e-01 \end{bmatrix}$
- Transfer vector T: $T = \begin{bmatrix} -9.4461e+01 \\ -2.6280e-01 \\ 1.8651e+01 \end{bmatrix}$
- Calibration Error: Camera1 = 4.4978e-01, Camera 2= 4.5000e-01, Stereo = 4.97791e-01

The components in the system are synchronized through triggers to ensure the acquired images from cameras are in the correct order with the projector's lighting pattern. (Fig. 7).

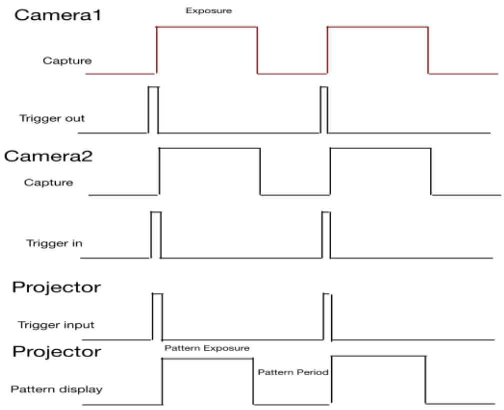

Figure 7. *Signal synchronizing trigger between cameras and projector.*

3.2. Results

Table 1. *Camera exposure setting values.*

No	1	2	3	4	5	6	7	8	9	10	11
Setting value (ms)	1/1000	1/500	1/250	1/125	1/60	1/30	1/15	1/8	1/4	1/2	1

Table 1 shows 11 different exposure time settings for the camera. With each exposure value, the camera will obtain images with different gray level intensity.

a) b)

Figure 8. *HDR image generated by (a) proposed method,(b) exposure fusion method.*

Fig. 8 shows that the gray level range when using the method in this paper (a) is better than the method using exposure fusion (b).

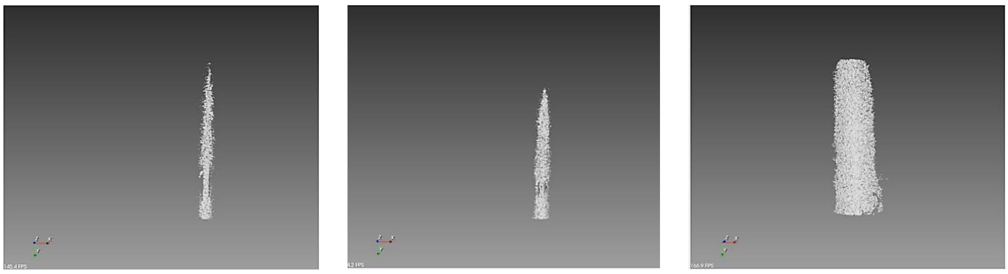

a) b) c)

Figure 9. *3D data obtained with (a) one exposure value,*
(b) exposure fusion method, (c) proposed method.

Fig. 9 shows the results of obtaining point cloud data by three different methods when performing high-gloss mechanical part scans. Fig. 9a using an exposure value of 16.66 ms records 1428 points in the point cloud, Fig. 9b uses exposure matching with a larger number of 3853 points, Fig. 9c uses the proposed method. The Fig. 9c shows that the proposed method can obtain 6364 points and the surface quality is guaranteed to be uniform.

The proposed method of using HDR produces more 3D points than the one that uses the single exposure value and exposure fusion. The execution time is also faster than the exposure fusion method (~120 s compared with 240 s). Therefore, with more data obtained, less surface undulation, the accuracy of the measurement is improved.

3.3. System Accuracy Evaluation

To evaluate the accuracy of the system, we used a standard template of the lengths which is the ceramic gauge/gage blocks grade 0 (from Mitutoyo), arranged in pairs of stairs with the standard length, respectively: **25**; **20.2**; **17.6**; **15** and **12.9** mm.

Fig. 10 shows how to arrange the sample bases in four steps on the optical table for the system to collect the 3D point cloud.

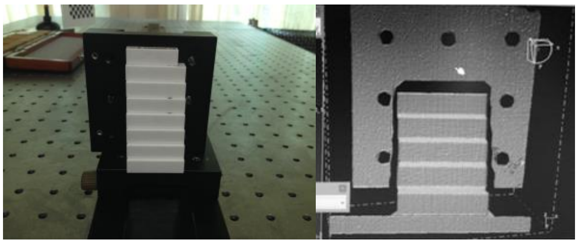

Figure 10. *Arrangement model of standard bases and obtained data.*

To measure the distance between the steps, Fig. 11-a shows how to create order planes from a set of selected points using the Gaussian best-fit method. First, we choose a point that lies above the second step, then project perpendicular to the plane created from the first step (Fig. 11-b), and do the same for the remaining steps (Fig. 11-c).

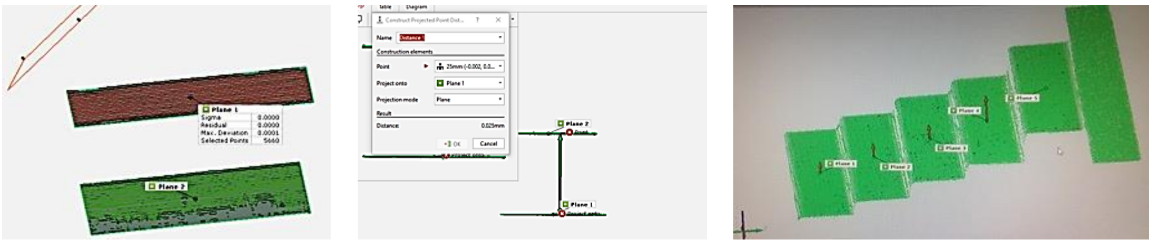

a) *b)* *c)*

Figure 11. *a) Generate a plane on the first step using Gom Inspect software with the largest deviation of 0.0001 mm with 5660 3D points selected, b) The measurement of the distance between a point on plane 1 and plane 2 is 25 mm, c) The plane by route method.*

Table 2. *Measurement results and deviation values.*

Real value(mm)	**1st**	**2nd**	**3rd**	**4th**	**5th**	**Sample standard deviation**	**Relative standard deviation**
4,800	4,802	4,801	4,799	4,798	4,799	0.0016	0.0015
2,600	2,601	2,602	2,599	2,599	2,598	0.0016	0.0015
2,600	2,600	2,601	2,598	2,598	2,599	0.0013	0.0012
2,100	2,101	2,090	2,099	2,100	2,098	0.0012	0.0011

Table 2 shows the results after five times of measuring four steps. The minimum standard deviation is 0.0012 mm when measuring steps with a distance of 2.1 mm and the highest is 0.0016 mm when measuring steps of 2.6 mm and 4.8 mm. The difference in measurement standard deviation is due to the influence of distortion of the optical system. The measurement positions at the optical center have smaller standard deviations than the measurement positions at the distance from the optical center.

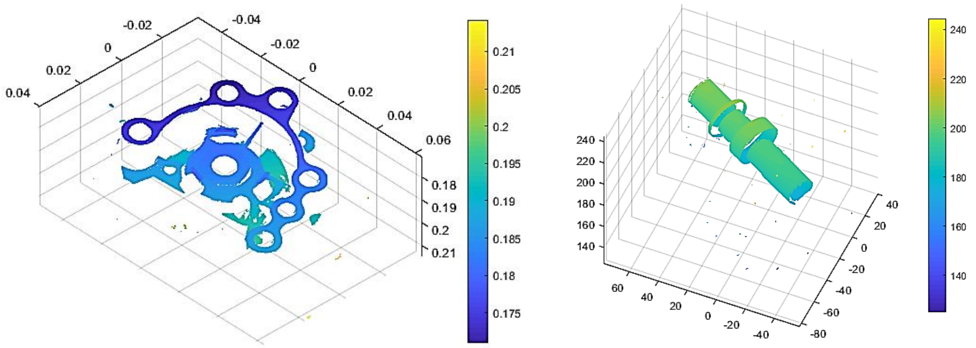

Figure 12. *3D scanned image example.*

4. CONCLUSIONS

This paper presented the experimental model for a 3D scanning system using gray code and line-shifting method. By synthesizing HDR images, the proposed method has enhanced the measurement data information for highly polished, complex surfaces of mechanical objects. Besides, the 3D data obtained by the proposed system is processed and measured using Gom Inspect software to determine the deviation of the smallest measurement of 0.0012 mm and a maximum of 0.0016 mm within the operating range of 180 ~ 250 mm distance from the device.

REFERENCES

[1]. Jens Gühring, *"Dense 3-D surface acquisition by structured light using off-the-shelf components"*, Proc. SPIE 4309, Videometrics and Optical Methods for 3D Shape Measurement, 220, 2000

[2]. S. S. Gorthi and P. Rastogi, *"Fringe projection techniques: whither we are?"* Optics and Lasers in Engineering, vol. 48, no. 2, pp. 133–140, 2010.

[3]. S. Zhang, *"Handbook of 3D Machine Vision: Optical Metrology and Imaging"*, CRC Press, Boca Raton, Fla, USA, 2013.

[4]. Jason Geng, *"Structured-light 3D surface imaging: a tutorial"*, Advances in Optics and Photonics, Vol. 3, Issue 2, 128-160, 2011

[5]. Lin, H., Gao, J., Zhang, G., Chen, X., He, Y., Liu, Y. *"Review and comparison of high-dynamic range three-dimensional shape measurement techniques,"* Journal of Sensors, 2017.

[6]. Hui Lin, Jian Gao, Qing Mei, Yunbo He, Junxiu Liu, and Xingjin Wang, *"Adaptive digital fringe projection technique for high dynamic range three-dimensional shape measurement,"* Opt. Express 24, 7703-7718, 2016

[7]. Lin, Hui, et al. *"Three-dimensional shape measurement technique for shiny surfaces by adaptive pixel-wise projection intensity adjustment."* Optics and Lasers in Engineering , 206-215, 2017

[8]. S. Feng, Y. Zhang,Q. Chen, C. Zuo, R. Li, and G. Shen, *"General solution for high dynamic range three-dimensional shape measurement using the fringe projection technique,"* Optics and Lasers in Engineering, vol. 59, pp. 56–71, 2014

[9]. H. Jiang, H. Zhao, and X. Li, *"High dynamic range fringe acquisition: a novel 3-D scanning technique for high-reflective surfaces,"* Optics and Lasers in Engineering, vol. 50, no. 10, pp.1484–1493, 2012

[10]. S. Zhang and S.-T. Yau, *"High dynamic range scanning technique,"* Optical Engineering, vol. 48, no. 3, Article ID 033604, 2009

[11]. G.-H. Liu, X.-Y. Liu, and Q.-Y. Feng, *"3D shape measurement of objects with high dynamic range of surface reflectivity,"* Applied Optics, vol. 50, no. 23, pp. 4557–4565, 2011

[12]. L. Ekstrand and S. Zhang, *"Auto exposure for three-dimensional shape measurement using a digital-light-processing projector,"* Optical Engineering, vol. 50, pp. 895 – 900, 2011.

[13]. S. K. Nayar, G. Krishnan, M. D. Grossberg, and R. Raskar, *"Fast separation of direct and global components of a scene using high frequency illumination"*, ACM Trans. on Graphics, 935-944, 2006

[14]. Daniel Moreno, Gabriel Taubin, *"Simple, Accurate, and Robust Projector-Camera Calibration"*, IEEE Second International Conference on, 464-471, 2012.

TÓM TẮT

ĐO BỀ MẶT 3D CỦA CHI TIẾT CƠ KHÍ BẰNG PHƯƠNG PHÁP ÁNH SÁNG CẤU TRÚC SỬ DỤNG GRAYCODE VÀ LINESHIFTING KẾT HỢP VỚI KỸ THUẬT ẢNH DẢI ĐỘNG MỞ RỘNG

Các chi tiết sau khi gia công cơ khí có bề mặt đặc trưng là độ tương phản hoặc độ bóng bề mặt cao. Một số phương pháp đo lường bằng quang học, bao gồm đo bề mặt 3D sử ánh sáng cấu trúc gặp khó khăn khi đo bề mặt dạng này. Bài báo này tập trung nghiên cứu phương pháp sử dụng kỹ thuật kỹ thuật ảnh dải động mở rộng (High Dynamic Range) cho các vân chiếu Graycode và lineshift nhằm nâng cao chất lượng đo bề mặt 3D. Nghiên cứu này xác định giá trị độ sáng tương ứng với độ phản xạ của từng điểm trên vật đo, thiết lập mô hình toán liên quan giữa giá trị thời gian phơi sáng của camera và giá trị điểm ảnh thu được để có thể đo các tọa độ điểm 3D bao gồm cả vùng bề mặt sáng chói và vùng tối. Mô hình thí nghiệm ánh sáng cấu trúc sử dụng dual-camera, máy chiếu lightcrafter 4500 được đồng bộ qua triggger, sử dụng vân chiếu Graycode và LineShifting.

Từ khóa: Ánh sáng cấu trúc; Graycode; LineShifting; Hệ thống đo 3D; Dải động mở rộng.

Received 16th May 2021
Revised 18th June 2021
Accepted 29th July 2021

Author affiliations:

[1]Department of Precision Mechanical and Optical Engineering, Hanoi University of Science and Technology;
[2]Center for Optoelectronics, National Center for Technological Progress;
[3]Hung Yen University of Technology and Education.
*Corresponding author: ngoctu@cfoc.vn.